

## Supplementary Material For

# A Novel La-Loaded Magnetic Hydrogel for the Deep Removal of Low-Concentration Fluoride Ions in Industrial Wastewater

Kaiyang Chen<sup>a</sup>; Ying Shen<sup>a</sup>; Ying Xu<sup>a</sup>; Jun Hu<sup>a</sup>; Jun Wang<sup>b</sup>; Yuchen Pang<sup>a</sup>; Zhaokai Tang<sup>a</sup>;

Chaoqun Tan<sup>a\*</sup>; Ming Chen<sup>c\*</sup>

*a School of Civil Engineering, Key Laboratory of Concrete and Prestressed Concrete Structures of  
the Ministry of Education, Southeast University, Nanjing 211189, China*

*b China Construction Industrial & Energy Engineering Group Co., Ltd., Nanjing 210023, China*

*c Department of Water Environment, Nanjing Research Institute of Ecological and Environmental  
Protection, Nanjing 210041, China*

**\*Corresponding author contact details:**

**Email: [tancq@seu.edu.cn](mailto:tancq@seu.edu.cn)**

**This supporting information contains:**

**35 Pages**

**6 Texts**

**14 Figures**

**11 Tables**

---

## List of captions

Text S1. Chemicals and Materials .....	1
Text S2. Detailed synthesis process of CH-Fe-MMT-La. ....	2
Text S3. Details of the characterizations for adsorbents.....	3
Text S4. Adsorption experiments .....	4
Text S5. Detection of F <sup>-</sup> . ....	5
Text S6. Details of the treatment of real F <sup>-</sup> -containing industrial wastewater based on precipitation-adsorption combined process .....	6
Figure S1. Detailed synthesis process of CH-Fe-MMT-La. ....	8
Figure S2. Effect of different materials on the removal of F <sup>-</sup> . ....	9
Figure S3. Effect of NaCMC dosage on the adsorption properties of adsorbents. ....	10
Figure S4. Effect of concentration of La(NO <sub>3</sub> ) <sub>3</sub> on the adsorption properties of hydrogels. ....	11
Figure S5. Effect of types of crosslinkers (a) and GA dosages (b) on the adsorption properties of hydrogels.....	12
Figure S6. Appearance and morphology of different adsorbent materials. ....	13
Figure S7. XRD patterns of MMT, NaCMC, Fe-MMT, and CH-Fe-MMT-La. ....	14
Figure S8. FTIR spectra of NaCMC, Fe-MMT, and CH-Fe-MMT-La. ....	15
Figure S9. TGA and DTG analyses of NaCMC, Fe-MMT, and CH-Fe-MMT-La .....	16
Figure S10. VSM analysis of CH-Fe-MMT-La.....	17
Figure. S11. Effect of initial F <sup>-</sup> concentrations on adsorption performance. ....	18
Figure. S12. Appearance and morphology of adsorbents at different pH conditions.....	19
Figure. S13. Thermodynamic fitting of adsorption at different initial F <sup>-</sup> concentrations. ....	20
Figure. S14. Effects of (a) Ca <sup>2+</sup> precipitation method and (b) Ca-F molar ratio on F <sup>-</sup> removal from real wastewater.....	21
Table S1. Main information of samples for real wastewater experiment .....	22
Table S2. Elemental composition of CH-Fe-MMT-La.....	23
Table S3. Adsorbent Swelling Test and La <sup>3+</sup> Leaching Test. ....	24
Table S4. The fitting parameters of CH-Fe-MMT-La for pseudo-first and pseudo-secondary kinetic models. ....	25
Table S5. The fitting parameters of CH-Fe-MMT-La for intra-particle kinetic models. ....	26
Table S6. Adsorption isotherm fitting parameters of CH-Fe-MMT-La for F <sup>-</sup> .....	27
Table S7. Mean adsorption free energy analysis based on D-R isotherm model .....	28
Table S8. Calculated results of adsorption thermodynamics .....	29
Table S9. Comparison of the adsorption performance of similar adsorbents in previous literatures for removing F <sup>-</sup> .....	30
Table S10. Working conditions and results for F <sup>-</sup> removal pre-experiments of real wastewater. ...	32
Table S11. Detailed conditions for real wastewater experiment. ....	34

---

## Text S1. Chemicals and Materials

Unless otherwise stated, all chemicals are of analytical purity (AR). Sodium fluoride (NaF), calcium chloride ( $\text{CaCl}_2$ ), calcium hydroxide ( $\text{Ca}(\text{OH})_2$ ), and sodium carboxymethylcellulose (NaCMC, with stickiness of 600-3000 mPa·s) were bought from Macklin Biochemical Technology Co. Ltd (Shanghai). Sodium chloride (NaCl), sodium sulphate ( $\text{Na}_2\text{SO}_4$ ), sodium carbonate ( $\text{Na}_2\text{CO}_3$ ), sodium bicarbonate ( $\text{NaHCO}_3$ ), iron (III) trichloride hexahydrate ( $\text{FeCl}_3 \cdot 6\text{H}_2\text{O}$ ), iron (II) sulfate heptahydrate ( $\text{FeSO}_4 \cdot 7\text{H}_2\text{O}$ ), and ethanol ( $\text{C}_2\text{H}_5\text{OH}$ ) were bought in Sinopharm Chemical Reagent Co. Ltd. Glutaraldehyde ( $\text{C}_5\text{H}_8\text{O}_2$ , GA, 25 wt.% solution in  $\text{H}_2\text{O}$ ), citrate ( $\text{C}_6\text{H}_8\text{O}_7$ , CA), lanthanum nitrate hexahydrate ( $\text{La}(\text{NO}_3)_3 \cdot 6\text{H}_2\text{O}$ ), trisodium citrate dihydrate ( $\text{Na}_3\text{C}_6\text{H}_5\text{O}_7 \cdot 2\text{H}_2\text{O}$ ), and sodium nitrate ( $\text{NaNO}_3$ ) were bought from Aladdin Scientific Co. Ltd. (Shanghai). Ca-based montmorillonite (MMT) was bought from Shanlinshiyu Mineral Products Company. Polymeric aluminum chloride (PAC,  $\text{Al}_2\text{O}_3\%$  = 10%) and polyacrylamide (PAM) were bought from Youquan Environmental Protection Technology Company.

---

**Text S2. Detailed synthesis process of CH-Fe-MMT-La.**

Magnetic montmorillonite particles were obtained by chemical co-precipitation of Fe(III) and Fe(II) in alkaline solution and then loaded on montmorillonite powder. In a typical synthesis process, 5.0 g of montmorillonite was put into 200 mL of NaOH solution ( $1.0 \text{ mol}\cdot\text{L}^{-1}$ ) for activation for 4 h. Firstly, 6.0 g of  $\text{FeCl}_3\cdot 6\text{H}_2\text{O}$  and 4.0 g of  $\text{FeSO}_4\cdot 7\text{H}_2\text{O}$  were dissolved in deionized water, and then added to the aforementioned solution. 30 min of ultrasonication was carried out to prevent the agglomeration. The pH of the mixture was adjusted to 10 ~ 12 and the black precipitate was collected after 1 h of reaction. After aging for 24 h, the precipitate was washed with deionized water and ethanol for 3 times and then dried in vacuum at 60 °C for 12 h. Then the brown powder was collected and grinded through a 100-mesh sieve to obtain the magnetic montmorillonite (Fe-MMT).

Next, 2.0 g of NaCMC was dissolved in 100 mL of distilled water, heated to 80 °C and stirred continuously to fully dissolve. 1.0 g of Fe-MMT dissolved in 25 mL of water and then mixed with the aforementioned NaCMC solution, stirred continuously for 1 h, after which, 2.0 wt.% of GA and 1.0 wt.% of CA were added, and stirred continuously for 1 h. The mixtures were left to rest for 2 ~ 12 h at room temperature. The mixtures were then squeezed into a  $0.05 \text{ mol}\cdot\text{L}^{-1}$   $\text{La}(\text{NO}_3)_3$  solution by a syringe to form microsphere hydrogel. The hydrogel was left to stand for 24 h and then washed with distilled water until the washing solution was neutral, and then dried under vacuum at 60 °C for 12 h. La-loaded magnetic hydrogel adsorbent (CH-Fe-MMT-La) was finally obtained.

---

### **Text S3. Details of the characterizations for adsorbents**

The microcrystalline structure and surface characteristics of catalysts were investigated by using a FEI Inspect F50 scanning electron microscopy (SEM) at an accelerated voltage of 20 kV. X-ray diffraction (XRD) measurements were recorded at room temperature using a Bruker D8-Discover advance X-ray powder diffractometer with Cu K $\alpha$  radiation and a scanning speed of 5° min<sup>-1</sup>. The scanning range of 2 $\theta$  was 4° to 90°. The accelerating voltage, wavelength and emission current were 40 kV, 1.5418 Å, and 40 mA, respectively. The X-ray photoelectron spectroscopy (XPS) of samples were obtained using the Thermo Fisher Scientific EscalLab 250Xi instrument with Al K $\alpha$  radiation and a beam spot size of 400  $\mu$ m, to investigate the elementary substance and the valence state. Full-spectrum analysis with a fluence of 100.0 eV and a scanning energy step of 1.0 eV, high-resolution scanning with a fluence of 20.0 eV and a scanning energy step of 0.1 eV. The fourier transform infrared (FTIR) spectrometer ranging from 4000-450 cm<sup>-1</sup> were analyzed by a Thermo Fisher Scientific Nicolet iS10 FT-IR spectrometer ranging from 1100-1000 cm<sup>-1</sup>. To get the thermal stability of the catalyst, the thermogravimetric analysis (TGA) and the derivative thermogravimetry (DTG) were carried out by a Mettler-Toledo TGA/DSC 3+ instrument with a heating rate of 10 °C·min<sup>-1</sup> and a temperature range of 20 to 1200 °C under N<sub>2</sub> atmosphere. The magnetic parameters of the adsorbent were measured using a vibrating sample magnetometer (VSM, 7404/8604, LakeShore, USA), with frequency of 12 Hz and magnetic field range of -20000 to 20000 Oe. A pore size analyzer (ASAP 2460, MicroActive, USA) was used to determine the specific surface area of the material was analyzed by the Brunauer-Emmett-Teller (BET) method. The pore size and pore volume were analyzed by the Barret-Joyner-Halenda equation. The working conditions: degassing temperature of 120°C and degassing time of 8 h.

---

#### **Text S4. Adsorption experiments**

Adsorption experiments were performed by adding adsorbent to a reactor containing a  $F^-$ -containing solution. The mixture was stirred at a constant stirring rate using a constant temperature water bath oscillation shaker, and single-variable-experiment were controlled (initial pH, initial concentration of  $F^-$ , adsorbent dosage, contact time, and co-existing anions) to obtain optimal operating conditions. After adsorption, the collected water samples were passed through a  $0.45\ \mu\text{m}$  filter membrane and the concentration of  $F^-$  was determined. Kinetic and thermodynamic characteristics of  $F^-$  adsorption processes were further analyzed.

---

**Text S5. Detection of F<sup>-</sup>.**

The concentration of F<sup>-</sup> was measured by the F<sup>-</sup> selective electrode method. Specifically, the concentration of F<sup>-</sup> was detected using a PXBJ-287 portable ion meter. When the fluoride ion electrode is in contact with the F<sup>-</sup>-containing test solution, the electric potential ( $E$ ) changes with the change of F<sup>-</sup>'s activity in the solution, obeying the Nernst equation (Eq. (S1)), and the fluoride ion electrode selected for this experiment has a measurement range of 0.05~1900 mg/L.

$$E_x = E_0 - \frac{2.303RT}{F} \log C_x \quad (S1)$$

where  $E_x$  represents the equilibrium potential of the sample to be measured, mV; while  $E_0$  is the zero potential value, mV.  $R$  is the universal ideal gas constant, which equals  $8.314 \text{ J}\cdot\text{mol}^{-1}\cdot\text{K}^{-1}$ .  $T$  is the thermodynamic temperature in kelvins, K;  $F$  is the Faraday's constant, which equals  $9.649 \times 10^7 \text{ J}\cdot\text{V}^{-1}\cdot\text{mol}^{-1}$ .  $C_x$  is the concentration of F<sup>-</sup>,  $\text{mg}\cdot\text{L}^{-1}$ .

---

**Text S6. Details of the treatment of real F<sup>-</sup>-containing industrial wastewater based on precipitation-adsorption combined process**

**Precipitation**

Nano Ca(OH)<sub>2</sub> (~0.8 μm diameter) was used for the precipitation experiments. A certain amount of wastewater sample and a certain amount of Ca(OH)<sub>2</sub> were added to the reactor (**Table S11**), and only the Ca-F molar ratio was adjusted without adjusting the pH. At the end of the reaction, the solution sample was taken from supernatant and then filtered through a 0.22 μm membrane to determine the residual F<sup>-</sup> concentration.

**Primary process**

The pH of water samples 1 and 2 was adjusted to 7.0, and water samples 3 and 4 were kept in an acidic pH environment. Nano Ca(OH)<sub>2</sub> with Ca-F molar ratio of 1.0 was then first added, and the solution pH was adjusted to 6.5~7.5 by stirring for 30 min at 150 r/min. After that, polymeric aluminum chloride (PAC) was added and stirred for 60 s. Finally, 0.1% wt. polyacrylamide (PAM) was added, and stirred for 30 min. After stirring for 60 s. After mixing all above reagents, the water samples were precipitated for 30 min and the supernatant was tested for the concentration of F<sup>-</sup>.

**Secondary process**

Take 900 mL of the supernatant effluent of primary process, for the secondary process F-removal. According to the F<sup>-</sup> concentration of the effluent, adding different dosages of CaCl<sub>2</sub> (Ca-F molar ratio of 0.5~0.75), PAC and PAM were then added in the order of the mixing process in primary process. At the end of coagulation and sedimentation, samples were taken to test the concentration of F<sup>-</sup>.

---

## **Adsorption**

Transfer 50 ml aliquots of supernatant from the effluent of secondary-process into reactors. The pH was adjusted to 6.0-7.0. Adsorption agent was added at **0.6 g** to **Sample 1** and **0.5 g** to **Samples 2, 3, and 4**. After reacting at 150 rpm for 4 hours at room temperature, samples were collected and tested after filtered with 0.45  $\mu\text{m}$  membranes.

**Figure S1. Detailed synthesis process of CH-Fe-MMT-La.**

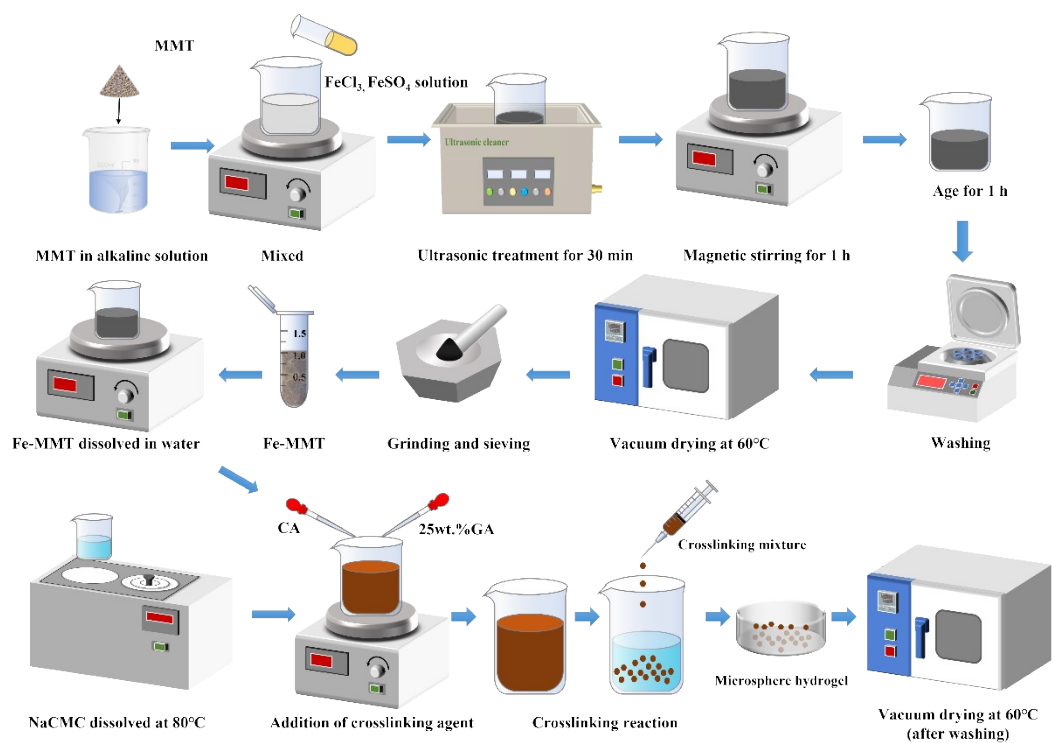
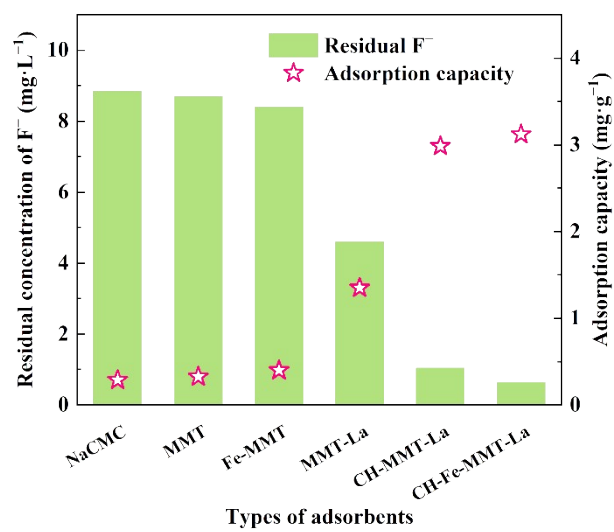
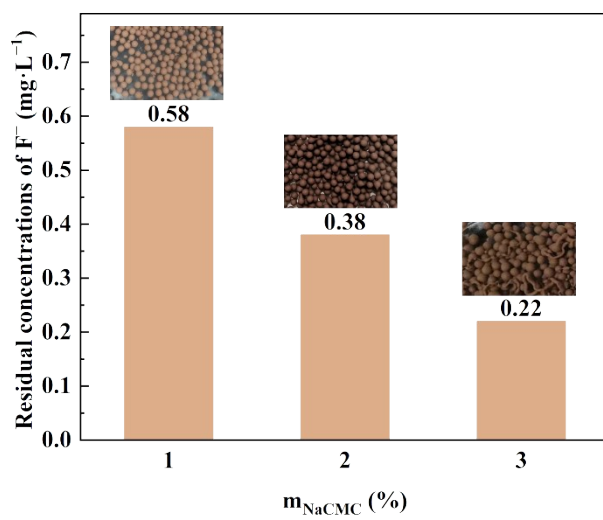


Figure S2. Effect of different materials on the removal of  $F^-$ .



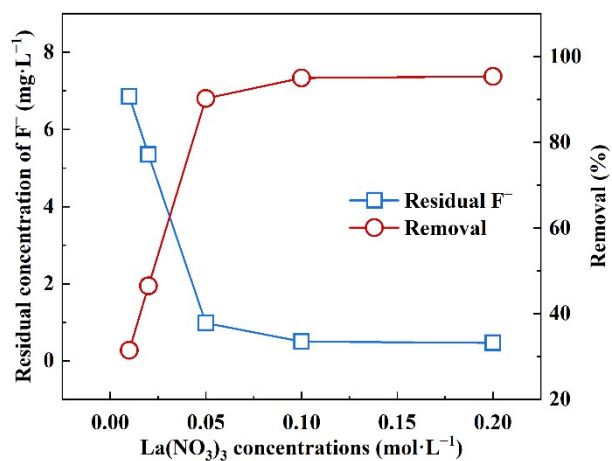
Working conditions: adsorbent:  $3.0 \text{ g} \cdot \text{L}^{-1}$ , stirring speed  $n = 150 \text{ rpm}$ ,  $T = 25 \text{ }^\circ\text{C}$ ,  $c(F^-)_0 = 10 \text{ mg} \cdot \text{L}^{-1}$ ,  $t = 4 \text{ h}$ .

**Figure S3. Effect of NaCMC dosage on the adsorption properties of adsorbents.**



Working conditions: adsorbent:  $2.0 \text{ g}\cdot\text{L}^{-1}$ ; stirring speed  $n = 150 \text{ rpm}$ ;  $T = 25 \text{ }^\circ\text{C}$ ;  $c(\text{F}^-)_0 = 10 \text{ mg}\cdot\text{L}^{-1}$ ,  $t = 4 \text{ h}$ .

Figure S4. Effect of concentration of  $\text{La}(\text{NO}_3)_3$  on the adsorption properties of hydrogels.

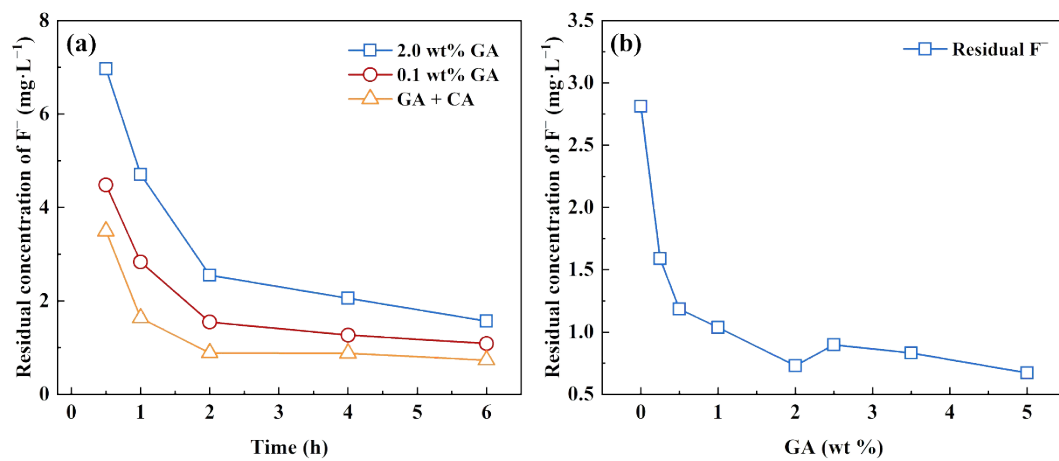


Working conditions: adsorbent: 2.0 g·L<sup>-1</sup>; stirring speed  $n = 150$  rpm;  $T = 25$  °C;  $c(\text{F}^-)_0 = 10$

mg·L<sup>-1</sup>,  $t = 4$  h.

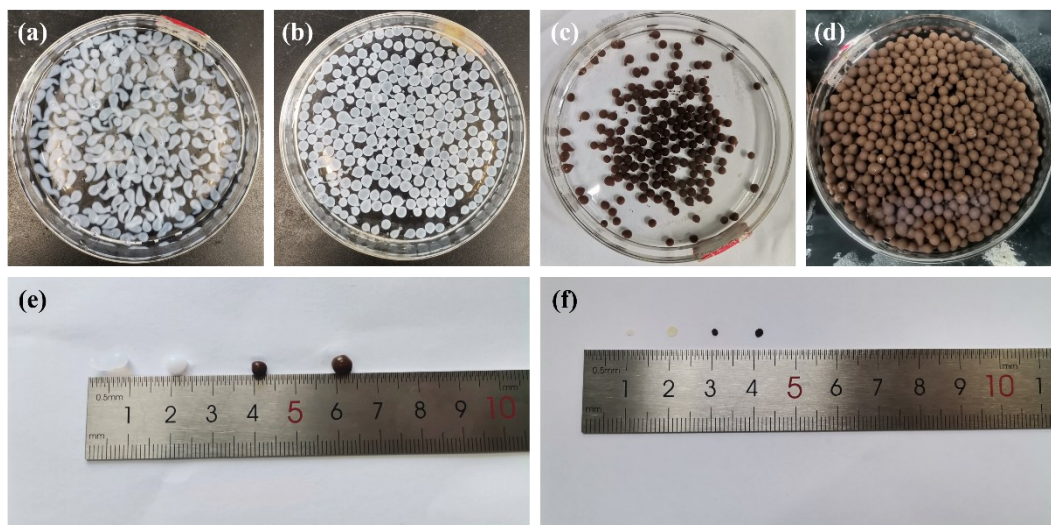
Figure S5. Effect of types of crosslinkers (a) and GA dosages (b) on the adsorption

properties of hydrogels.



Working conditions: adsorbent:  $3.0 \text{ g}\cdot\text{L}^{-1}$ ; stirring speed  $n = 150 \text{ rpm}$ ;  $T = 25 \text{ }^\circ\text{C}$ ;  $c(F^-)_0 = 10 \text{ mg}\cdot\text{L}^{-1}$ ;  $t = 4 \text{ h}$  (only for **Figure S5b**).

**Figure S6. Appearance and morphology of different adsorbent materials.**



(a) CH-La; (b) CH-La & GA+CA; (c) CH-Fe-MMT-La; (d) CH-Fe-MMT-La & GA+CA; (e) size of the wetted state; (f) size of the dry state.

Figure S7. XRD patterns of MMT, NaCMC, Fe-MMT, and CH-Fe-MMT-La.

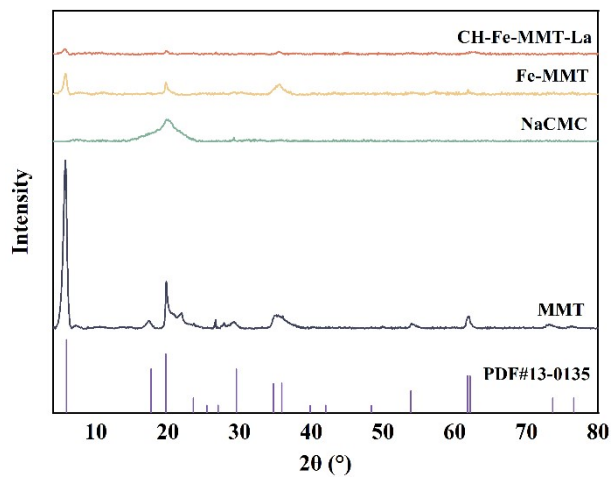


Figure S8. FTIR spectra of NaCMC, Fe-MMT, and CH-Fe-MMT-La.

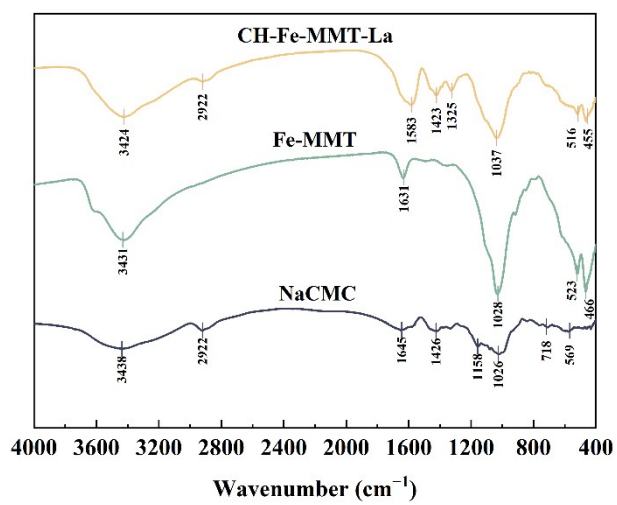


Figure S9. TGA and DTG analyses of NaCMC, Fe-MMT, and CH-Fe-MMT-La

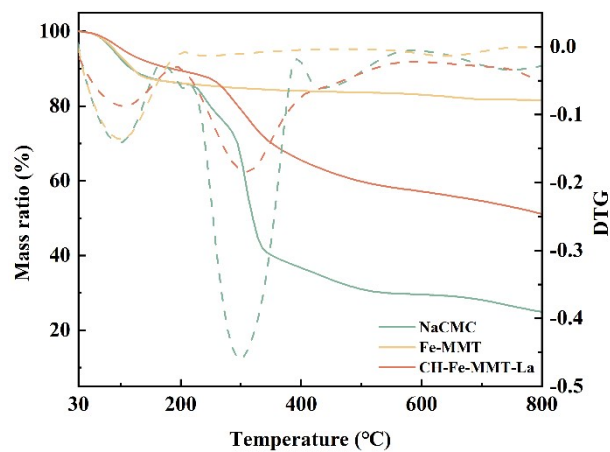


Figure S10. VSM analysis of CH-Fe-MMT-La.

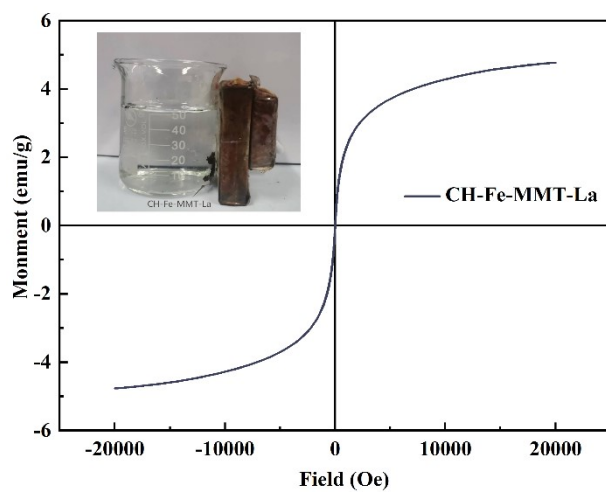
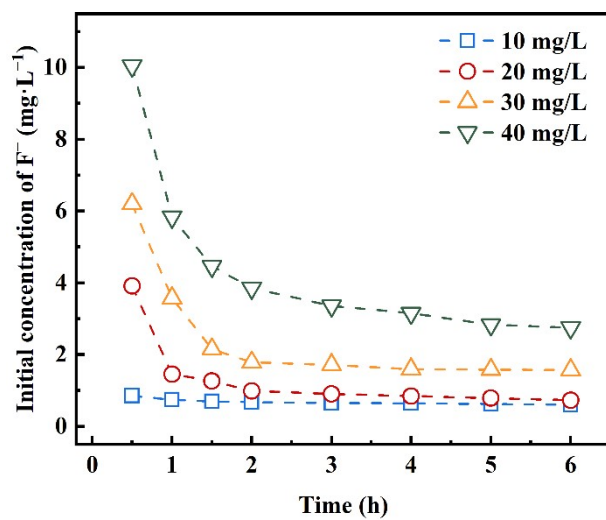


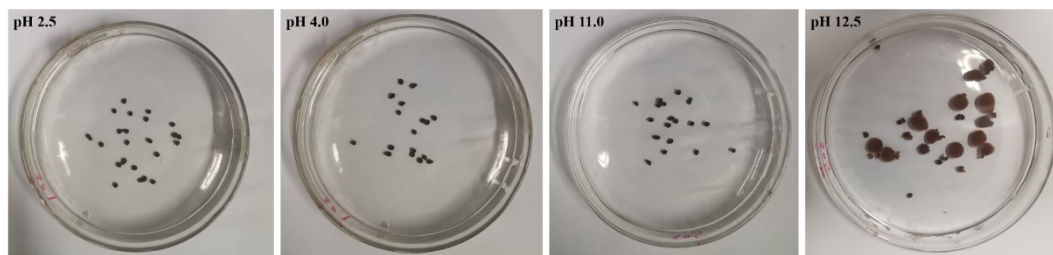
Figure. S11. Effect of initial  $F^-$  concentrations on adsorption performance.



Working conditions: adsorbent:  $3.0 g \cdot L^{-1}$ ; stirring speed  $n = 150$  rpm;  $T = 25^\circ C$ .

---

**Figure. S12. Appearance and morphology of adsorbents at different pH conditions.**



Working conditions: adsorbent: 30 mg; volume of solution: 50 ml;  $t = 24$  h;  $T = 25^{\circ}\text{C}$ .

Figure. S13. Thermodynamic fitting of adsorption at different initial  $F^-$  concentrations.

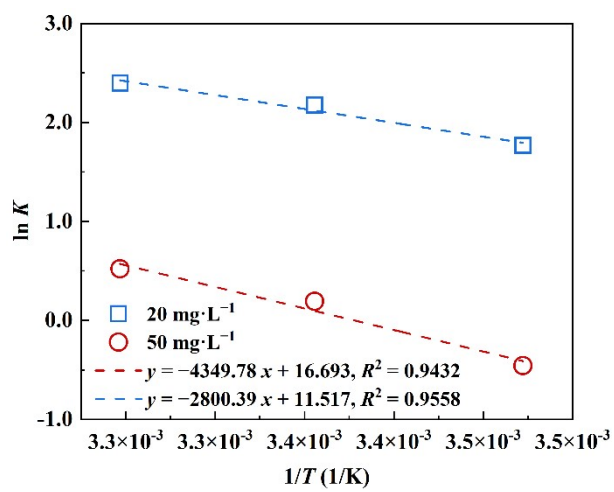
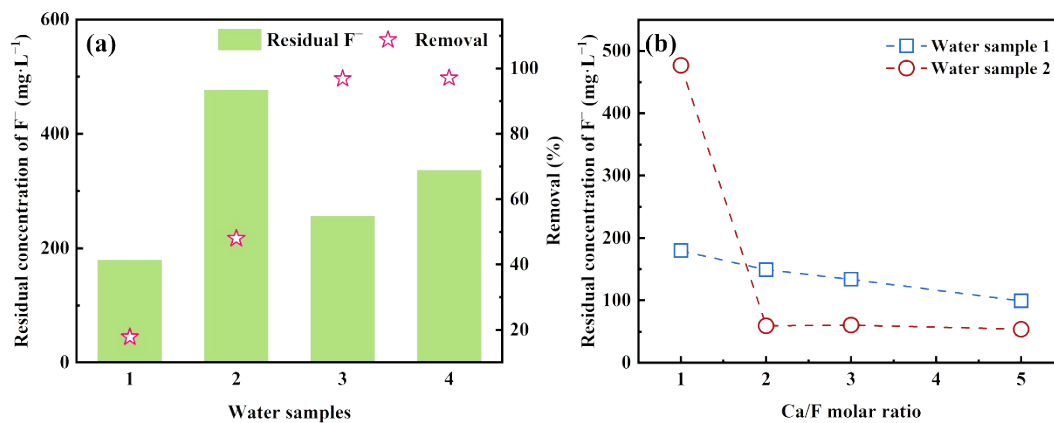


Figure. S14. Effects of (a)  $\text{Ca}^{2+}$  precipitation method and (b) Ca-F molar ratio on  $\text{F}^-$  removal from real wastewater



Working conditions: reaction time  $t_1 = 30$  min, precipitation time  $t_2 = 30$  min, stirring speed  $n = 150$  r/min, temperature  $T = 25 \pm 5$  °C.

---

**Table S1. Main information of samples for real wastewater experiment**

<b>Samples</b>	<b>pH</b>	<b>F<sup>-</sup> (mg·L<sup>-1</sup>)</b>	<b>COD (mg·L<sup>-1</sup>)</b>
Sample 1	11.0	218.7	1550
Sample 2	8.8	916.2	6100
Sample 3	4.0	8169.0	4500
Sample 4	5.0	11604.0	560

**Samples 1** and **2** were taken from the production wastewater emitted from a Li-battery production enterprise in Nanjing, Jiangsu Province, China. **Samples 3** and **4** were taken from the production wastewater of an electroplating industry enterprise in Nanjing, Jiangsu Province, China.

---

**Table S2. Elemental composition of CH-Fe-MMT-La**

---

<b>Elements</b>	<b>Percentage by weight (%)</b>	<b>Percentage of atomic numbers (%)</b>
C	13.13	39.34
O	11.77	26.49
Fe	15.02	9.68
La	51.51	13.35
Si	1.53	2.05
Al	6.70	8.58
Ca	0.00	0.00
Na	0.33	0.52

---

---

**Table S3. Adsorbent Swelling Test and La<sup>3+</sup> Leaching Test.**

---

<b>Water quality indicators</b>	<b>Before adsorption</b>	<b>After reaction</b>
Concentration of F <sup>-</sup> (mg·L <sup>-1</sup> )	20.0	0.73
pH	6.9	5.4
COD (mg·L <sup>-1</sup> )	<3	12
<b>La<sup>3+</sup> (μg·L<sup>-1</sup>)*</b>	<b>0</b>	<b>5.01</b>
<b>Swelling rate (g/g)</b>	<b>\</b>	<b>0.62</b>

---

\* The concentration of La<sup>3+</sup> after adsorption reaction was determined by inductively coupled plasma optical emission spectroscopy (ICP-OES, SPECTROBULUE, Germany).

**Table S4. The fitting parameters of CH-Fe-MMT-La for pseudo-first and pseudo-secondary kinetic models.**

$c(F^-)_0$ ( $\text{mg}\cdot\text{L}^{-1}$ )	Pseudo-first kinetic model			Pseudo-secondary kinetic model		
	$K_1(\text{min}^{-1})$	$q_e(\text{mg}\cdot\text{g}^{-1})$	$R^2$	$K_2(\text{g}/(\text{mg}\cdot\text{min}))$	$q_e(\text{mg}\cdot\text{g}^{-1})$	$R^2$
20	0.2847	6.183	0.8428	0.0351	6.489	0.9999
50	0.1409	12.495	0.9650	0.0072	13.387	0.9999

---

**Table S5. The fitting parameters of CH-Fe-MMT-La for intra-particle kinetic models.**

---

$c(\text{F}^-)_0$ ( $\text{mg}\cdot\text{L}^{-1}$ )	Stage 1			Stage 2			Stage 3		
	$K_{d1}$	$C_i$	$R^2$	$K_{d2}$	$C_i$	$R^2$	$K_{d3}$	$C_i$	$R^2$
20	0.458	2.776	0.969	0.034	5.931	0.867	0.007	6.279	0.984
50	1.540	1.126	0.947	0.318	9.034	0.983	0.054	11.955	0.907

---

---

**Table S6. Adsorption isotherm fitting parameters of CH-Fe-MMT-La for F<sup>-</sup>**

Temperatur <b>e</b>  <b>(K)</b>	Langmuir model			Freundlich model		
	$q_m(\text{mg}\cdot\text{g}^{-1})$	$K_L(\text{L}\cdot\text{mg}^{-1})$	$R^2$	n	$K_F(\text{mg}\cdot\text{g}^{-1})$	$R^2$
288	11.861	0.598	0.9982	6.148	6.502	0.9514
298	16.059	0.732	0.9961	4.884	8.168	0.8091
308	16.912	0.895	0.9982	4.735	8.735	0.8290

---

---

**Table S7. Mean adsorption free energy analysis based on D-R isotherm model**

---

<b>Temperature (K)</b>	<b><math>K_e</math> (mol<sup>2</sup>·kJ<sup>-2</sup>)</b>	<b><math>q_m</math> (mg·g<sup>-1</sup>)</b>	<b><math>E</math> (kJ·mol<sup>-1</sup>)</b>	<b><math>R^2</math></b>
288	0.0018	17.299	16.67	0.9726
298	0.0022	30.209	15.04	0.8784
308	0.0019	29.942	16.05	0.8700

---

---

**Table S8. Calculated results of adsorption thermodynamics**

---

$c(\text{F}^-)_0$	Temperature (K)	$\Delta G$ (kJ·mol <sup>-1</sup> )	$\Delta H$ (kJ·mol <sup>-1</sup> )	$\Delta S$ (kJ·mol <sup>-1</sup> ·K <sup>-1</sup> )
	288	-4.23		
20	298	-5.39	23.28	0.096
	308	-6.14		
	288	1.10		
50	298	-0.48	36.16	0.122
	308	-1.33		

---

**Table S9. Comparison of the adsorption performance of similar adsorbents in previous literatures for removing F<sup>-</sup>.**

Adsorbent	pH	Temperature (K)	Dosages (g·L <sup>-1</sup> )	Time	$c(F^-)_0$ (mg·L <sup>-1</sup> )	$q_{max}$ (mg·g <sup>-1</sup> )	Reference
La-Ca/CG-SA	6.0	298	0.3	10.0 h	3.0	15.7	1
3D crosslinked chitosan	3.0~12.0	298	50	1.0 h	797.1	64.7	2
La(COOH) <sub>3</sub>	2-9	303	0.2	100 min	10-80	245.02	3
Polymeric hydrogels modified with FeCl <sub>3</sub>	6.7	298	10.0	12.0 h	4.0	0.342	4
Fe <sub>3</sub> O <sub>4</sub> -Al <sub>0.94</sub> La <sub>0.06</sub> O <sub>1.5</sub> -Ca- ALG	7.0	298	20.0	24.0 h	10.0	132.3	5
Gamma degraded chitosan- Fe(III) beads	4.0	303	8.0	30 min	25.0	45.45	6
MCH-La	3.0~10.0	298	0.3	10 min	20.0	136.78	7

<b>Adsorbent</b>	<b>pH</b>	<b>Temperature (K)</b>	<b>Dosages (g·L<sup>-1</sup>)</b>	<b>Time</b>	<b><math>c(F^-)_0</math> (mg·L<sup>-1</sup>)</b>	<b><math>q_{\max}</math> (mg·g<sup>-1</sup>)</b>	<b>Reference</b>
(net-CS)-g-NVCL/DMAAm	7.68	298	2.0	50.0 h	0.9	0.150	8
Zr-alginate-carrageenin hydrogel	2.0~8.0	298	20.0	60 min	200.0	41.66	9
<b>CH-Fe-MMT-La</b>	<b>3.0~7.0</b>	<b>298</b>	<b>3.0</b>	<b>4.0 h</b>	<b>50</b>	<b>16.06</b>	<b>This study</b>

**Table S10. Working conditions and results for F<sup>-</sup> removal pre-experiments of real wastewater.**

Water sample and its $c(\text{F}^-)_0$	Working conditions	Volume of water	Dosages*			Effluent	
			Ca <sup>2+</sup> (g·L <sup>-1</sup> )	PAC (mg·L <sup>-1</sup> )	PAM (mg·L <sup>-1</sup> )	pH	Residual $c(\text{F}^-)$
Water sample 1 (218.7 mg·L <sup>-1</sup> )	Precipitation	1000 mL of raw water	0.85	0	0	9.8	153.06
	Primary process	1000 mL of raw water	0.85	100	1.0	7.56	83.58
	Secondary process	900 mL of supernatant	0.36	100	1.0	7.36	45.15
Water sample 2 (916.2 mg·L <sup>-1</sup> )	Precipitation	1000 mL of raw water	3.58	0	0	12.9	248.8
	Primary process	1000 mL of raw water	3.58	100	1.0	7.8	60.94
	Secondary process	700 mL of supernatant	0.27	100	1.0	7.54	31.76
Water sample 3 (8169 mg·L <sup>-1</sup> )	Precipitation	200 mL of raw water	31.82	0	0	13.12	336.4
	Primary process	1000 mL of raw water	31.82	400	1.0	11.82	108.0
	Secondary process	700 mL of supernatant	0.32	100	1.0	11.76	104.1

---

Water sample 4 (11604 mg·L <sup>-1</sup> )	Precipitation	200 mL of raw water	45.2	0	0	13.0	256.4
	Primary process	1000 mL of raw water	45.2	800	1.0	11.65	128.2
	Secondary process	900 mL of supernatant	0.37	100	1.0	11.44	119.2

---

\*: The dosage of Ca<sup>2+</sup> is calculated according to the actual dosages of Ca(OH)<sub>2</sub> or CaCl<sub>2</sub>, while the dosage of PAC is calculated according to the active ingredient of

Al.

**Table S11. Detailed conditions for real wastewater experiment.**

Water samples	Primary process			Secondary process			Adsorption
	n (Ca/F)	PAC (mg·L <sup>-1</sup> )	PAM (mg·L <sup>-1</sup> )	n (Ca/F)	PAC (mg·L <sup>-1</sup> )	PAM (mg·L <sup>-1</sup> )	CH-Fe-MMT-La (mg·L <sup>-1</sup> )
1	1.0	400	2.0	0.5	200	1.0	12.0
2	2.0	400	2.0	0.5	100	1.0	10.0
3	0.75	600	2.0	0.5	200	1.0	10.0
4	0.75	800	2.0	0.5	100	1.0	10.0

---

## References

1. Y. Xu, Z. Wang, Z. Wu, X. Li, X. Bi, G. Feng and N. Li, Lanthanum-calcium modified coal gangue-alginate composite hydrogel beads for efficient fluoride removal from groundwater, *Inorg. Chem. Commun.*, 2026, **185**, 116101.
2. F. Liu, Q. Wang, Y. Li, Z. Zhou, N. Wang, T. Wang, X. Huang and H. Hao, 3D crosslinked chitosan for fluoride remediation in industrial wastewater: From structure to performance enhancement, *Sep. Purif. Technol.*, 2025, **360**, 131070.
3. W. Yang, F. Shi, W. Jiang, Y. Chen, K. Zhang, S. Jian, S. Jiang, C. Zhang and J. Hu, Outstanding fluoride removal from aqueous solution by a La-based adsorbent, *RSC Adv.*, 2022, **12**, 30522-30528.
4. V. Rosendo-González, E. Gutiérrez-Segura, M. Solache-Rios and A. Amaya-Chavez, Polymeric hydrogels for the removal of fluoride ions from natural water and its toxicity, *Desalin. Water Treat.*, 2025, **321**, 100974.
5. H. Basu, M. Amarnath, B. Modak, H. Parab, R. Basu, S. Goyal, S. Saha, S. Singh and C. N. Patra, Development of magnetic La doped Al<sub>2</sub>O<sub>3</sub> core-shell nanoparticle loaded hydrogel for selective recovery of fluoride from aquatic medium, *Chemosphere*, 2024, **353**, 141504.
6. S. Tandekar, D. Saravanan, S. Korde and R. Jugade, Gamma degraded chitosan-Fe(III) beads for defluoridation of water, *Mater. Today*, 2020, **29**, 726-732.
7. S. Dong and Y. Wang, Characterization and adsorption properties of a lanthanum-loaded magnetic cationic hydrogel composite for fluoride removal, *Water Res.*, 2016, **88**, 852-860.
8. J. C. Burillo, L. Ballinas, G. Burillo, E. Guerrero-Lestarjette, D. Lardizabal-Gutierrez and H. Silva-Hidalgo, Chitosan hydrogel synthesis to remove arsenic and fluoride ions from groundwater, *J. Hazard. Mater.*, 2021, **417**, 126070.
9. A. Srivastava, M. Kumari and K. S. Prasad, Hydrogel beads containing ginger extract mediated nano-zirconium as an adsorbent for fluoride removal from aqueous solution, *Int. J. Environ. Anal. Chem.*, 2023, **103**, 1572-1586.